TECHNICAL BULLETIN T-143
OCTOBER 1976
OKLAHOMA STATE UNIVERSITY ● EXPERIMENT STATION

Oscillatory Transpiration in a Cotton Plant: An IBM/CSMP Computer Simulation

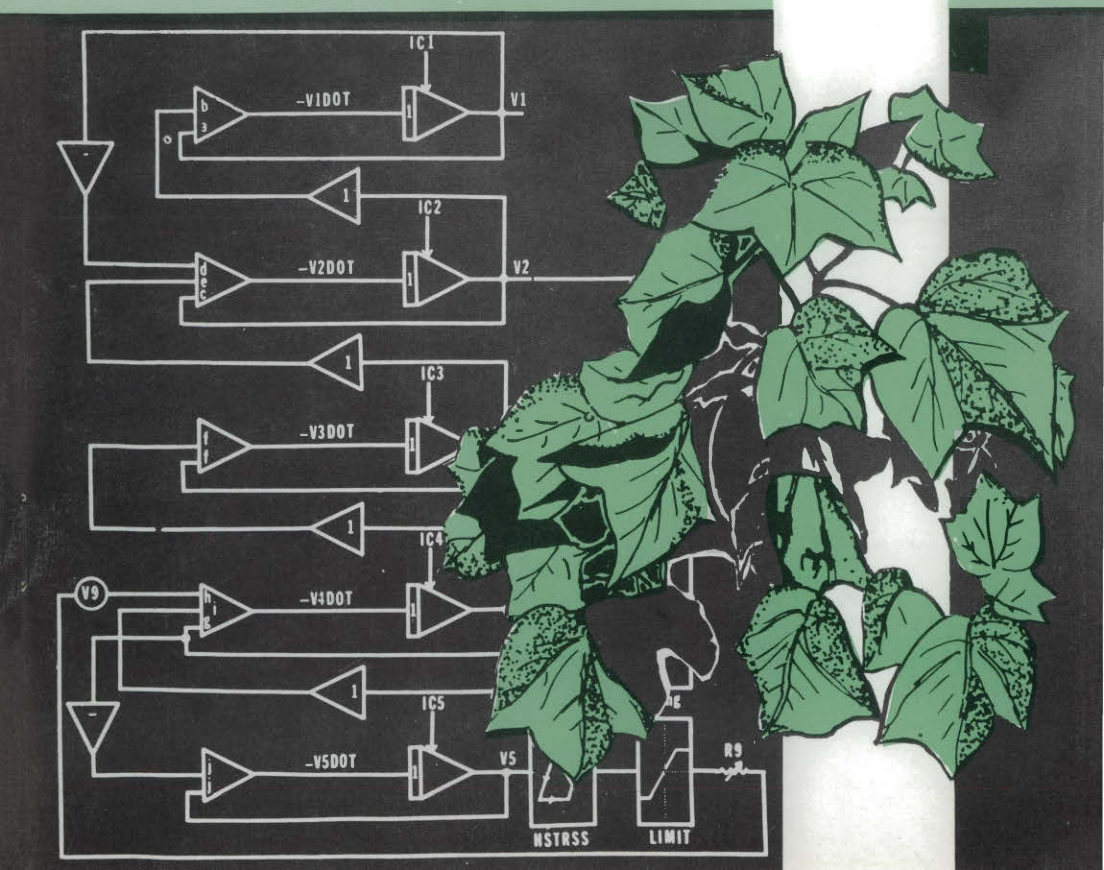

Oscillatory Transpiration in a Cotton Plant: An IBM/CSMP Computer Simulation

G. A. Shirazi, J. F. Stone, and C. M. Bacon*

Cyclic variations in transpiration and other concurrent and related plant functions have been reported in the literature for over a decade (1). The oscillations take place even if environmental conditions of light and temperature are constant. Researchers have used modeling to help explain the phenomena. This has been possible because in recent years there has been wide acceptance of the analogy between the flow of electricity through a conductor and that of water flow through the plant-atmosphere pathway. It is assumed that the movement of water through the plant and into the air is proportional to the gradient in water potential, which is the driving force, and is inversely proportional to the resistance in the pathway.

Barrs (1) cited several types of models used to simulate oscillatory flow in plants. Some of these involved first-order systems as well as second-order systems. Analogies ranging from mass-spring to transmission lines have been proposed to describe the water flow mechanics in plants. Shirazi (11) reported that most models found in the literature are of limited application to the whole plant, being either over-complicated, unrealistic or too specific with respect to a plant component.

They derived a model which was simple, realistic and generalized in its functioning. It was based on synoptic measurements made on several variables and parameters relating to water uptake, flow and retention during oscillatory transpiration of cotton (*Gossypium hirsutum L.*, cv Stoneville 7A) in a growth chamber. Roots were continuously aerated and measurements provided data on the behavior of the plant and several variables through the entire daylight period. The relationship

*Former Graduate Research Assistant and Professor, respectively, Department of Agronomy; Professor, Department of Electrical Engineering, Oklahoma State University. The senior author is presently Chief, Water Quality Division, Oklahoma Water Resources Board, Oklahoma City, Oklahoma.

The authors wish to thank Dr. Robert J. Mulholland, Professor Paul A. McCollum, both of the Electrical Engineering Department, and Dr. L. P. Varga, Chemistry Department, for their valuable suggestions throughout the course of the study.

The research reported herein was conducted under Oklahoma Station Project 1398-H.

between stomatal action and leaf water potential was hysteretic and reproducible. These experimental data were sufficient to furnish values of initial conditions, parameters and ranges of variation to operate a simple conceptual model of the oscillatory system. The model was simple, realistic and generalized in its functioning. It was based upon the model of Lang (6). The model also incorporated the results and observations of Skidmore (12) in conjunction with information available in the contemporary literature. It conceptualized a coupling between guard cell and stomatal resistance capable of producing either damped or sustained oscillations.

The purpose of this bulletin is to implement the model of Shirazi (9) on a digital computer using the Continuous System Modeling Program (CSMP) language which is available on IBM-1130 and 360 computers. The language allows a worker to concentrate on the biological phenomenon of interest rather than the intricacies of numerical analysis. This simulation model and the corresponding computer program is described in detail for those who wish to use the model.

The Model

The model is divided into components which simulate the continuum of the transpiration pathway in a plant (Figure 1). Each component is composed of one or more resistances and a capacitance simulating the corresponding functional relationships in the plant. This model is similar to Lang (6), except that this one has variable root resistance (R_1 and R_2) and added variable gaseous resistance (R_g) in series with stomatal resistance (R_s). Cuticular resistance is not shown in the model since only an insignificant amount of water is lost through that pathway. Capacitances are shown to be of constant magnitude and the system dynamics is initiated by an evaporative demand simulated by constant potential E. A feedback mechanism governing the action of guard cell potential and stomatal resistance is represented by a coupling shown as blocks labeled HSTRSS and LIMIT. The nature of the coupling and its function was detailed by Shirazi (9). It furnishes a delayed, hysteresis related feedback coupling consistent with the observations of Shirazi (11).

In the root component, workers (1, 7, 10, 12) have shown root resistance to vary during the photoperiod and also diurnally. Hence, variable root resistance R_1 and R_2 are introduced in the model. Shirazi. (10) showed root resistance to be time and pressure dependent, and suggested an equation for its representation. A certain amount of storage simulated by the capacitance (C_1) is included in that component. The inclusion of C_1 is in agreement with Lang (6) and Hopmans (3). R_3+R_4 is the stem and petiole resistance. C_2 is the capacitance of those com-

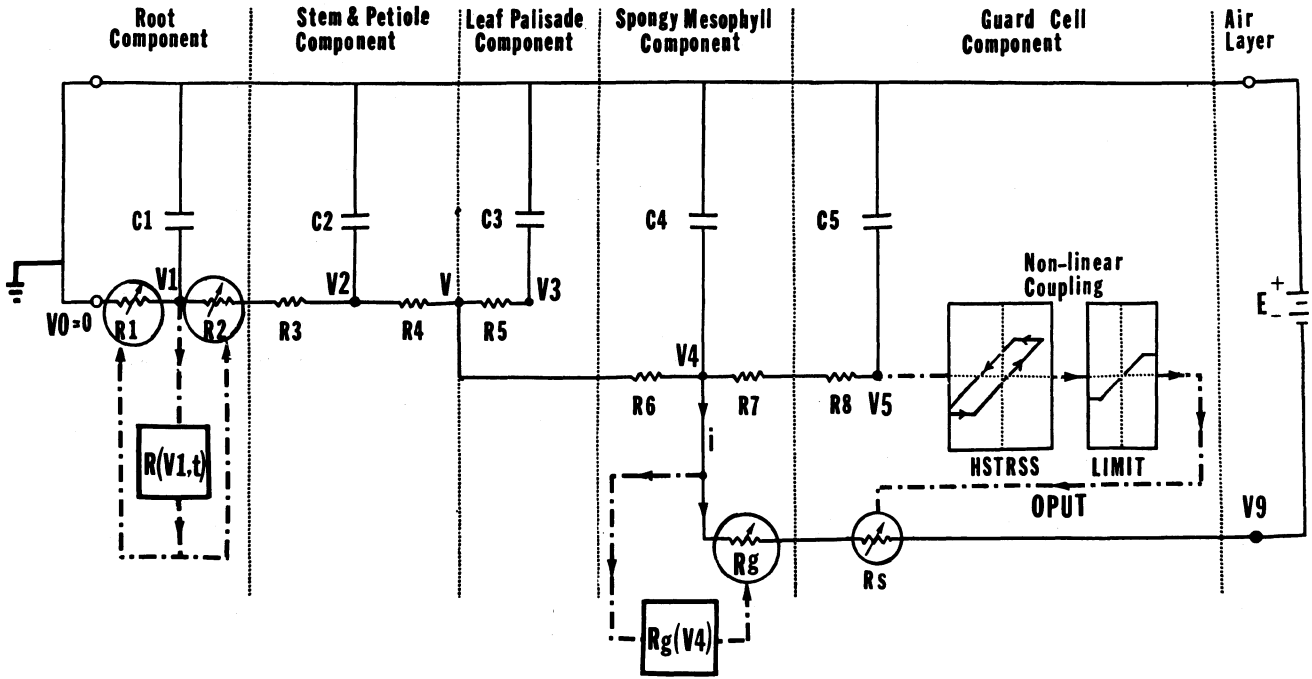

Figure 1. Electric analog model of the oscillatory transpiration in a cotton plant. Roots are in nutrient solution (assumed at zero potential). The model is driven by a constant input (E). Oscillations are governed by the nonlinear coupling in the guard cell component.

ponents. R_5 is the resistance in the leaf palisade and C_3 is the capacitance there. R_6 and R_7 are resistances to flow in the spongy mesophyll component with C_4 as capacitance. R_8 and C_5 are resistance and capacitance in the guard cells. R_g and R_s are resistance to the gaseous phase loss of water from the leaves. R_g is resistance in the conversion of liquid to gas and allows for phase change (9). R_s is resistance due to the degree of closure of the stomata. Instead of trying to model each leaf independently, the model assumes one lumped value for each major component (9).

Evaporative resistance (R_g) depends upon changes in potential largely in mesophyll component. Thus, a closed loop path describes the interdependence of gaseous resistance and potential changes in this component. The water balance of the leaf depends upon the stomatal resistance (R_s), but stomatal aperture, which governs its resistance, depends upon leaf water potential. Thus, leaf water balance results from a control system with negative feedback.

In their model Lang (6) pointed out a possible coupling between the guard cell potential and the stomatal resistance. They did not mention the nature of this coupling and emphasized that their model would not oscillate. Thus, their model did not describe the dynamic behavior of oscillatory transpiration. Assignment of values to these components is examined in detail by Shirazi (9).

Lang (6) indicated that a model of this design could show oscillation in flow by adding a proper number of resistance-capacitance units. This had to be checked in the present model prior to assigning values to components. Overlooking a proper assignment of R-C units could invalidate the entire model.

The network model in Figure 1 contains five capacitors and can be mathematically described by a system of five first-order nonlinear differential equations. The behavior of the model is determined by the nonlinear relations for R_1, R_2, R_g and R_s. Because of its nonlinear properties, the model is most easily analyzed by computer simulation techniques. However, certain approximations can be made by direct calculation to establish estimates of the network time constants and parameters associated with the oscillations.

If the charging and discharging cycles are separated and constant values of R_1, R_2, R_g and R_s established during these cycles, then the model differential equations become linear and the values of fixed time constants can be found. Since the model is fifth-order, five time constants are available to the modeler. From the theory of linear R-C networks (5), it can be shown that no oscillation of the network variables can occur, regardless of the number of R-C pairs added to the network, contrary to the statement by Lang (6). Thus, the oscillations must be produced by the nonlinear coupling of R_g and R_s to the potentials V_4 and V_5 in

Figure 1. It then follows that the period of oscillation is controlled by the switching of the resistance $R_9 = R_g + R_s$. The speed of response of the network variables, after a switching has occurred, depends upon the network time constants (a function of the resistors and capacitors). These concepts are applied in the following discussion.

With these values of resistance and capacitance, the five time constants of the network were evaluated for the charging and discharging transients. Fixed values of R_1, R_2, R_g and R_s for the two transient conditions were assumed. A 5 X 5 matrix containing 25 elements (Table 1) was derived from coefficients of the five simultaneous differential equations in the "state variables" V_i, $i = 1, 2, 3, 4, 5$. From this matrix, sets of eigenvalues were calculated for the charging and discharging conditions (See Appendix 3). All eigenvalues were found to be real and negative, for all three cases, thus assuring stability of the linearized model. The dominant time constant was found to be approximately equal to 10 minutes in both cases. This value is larger than expected, but it must be remembered that the model is actually nonlinear and that the nonlinear couplings alter the effective values of the time constants substantially. Thus, the frequency of oscillation is dictated more by the nature of the nonlinear couplings than by the values of the time constants of the linearized model.

Simulation Model

Development of the State Equations

As indicated, the various plant components are visualized as an electric network consisting of elements of resistance and capacitance. E is the driving force simulating the constant evaporative demand.

Equating the Ohm's law definition of current with the time-variant current in an ideal capacitor, state equations of the following general form were obtained,

$$(1) \qquad \frac{dV}{dt} = \frac{V(t)}{RC}$$

where V is potential on the capacitor, R is resistance of the pathway, and C is the capacitance. Equation 1 describes the dynamics of the potential change in the capacitor. According to the Kirchhoff's law of nodal analysis, the algebraic sum of flows at a node from all its branches is zero. A convention followed in the present analysis is that the incoming flow at a node is positive and the outgoing flow is negative. Also,

since the evaporative demand is simulated as a negative water potential, the driving force, E, is also negative. This approach is consistent with the concept that during transpiration water potential in all plant components is negative.

Accordingly, state equations were developed for each plant component shown in Figure 1. Equation 2 describes the dynamics of the potential change in root component at the node.

$$(2) \quad \frac{dV_1}{dt} = -[(V_1 - V_2) / (R_2C_1 + R_3C_1) + V_1/(R_1C_1)]$$

The time-constants R_1C_1 and R_2C_1 were equal since the capacitance was modeled at the midpoint of the root resistance. The use of time-variant root resistance is consistent with the data reported and concept advanced by several workers (7, 8, 10, 12).

Shirazi (10) have given a quantitative estimate of the root resistance at different time of the photoperiod. They reported a 3- to 5-fold increase in the root resistance from early morning to late evening. From that analysis a time-dependent equation for average slope of the line plotted on a semi-log scales of water uptake versus applied suction was obtained as follows

$$(3) \quad \text{UPTAKE} = \exp[2.303\ (\bar{A} + K(t)\tau)]$$

where τ is the applied suction in the roots, A is average uptake intercept and K(t) is the time-variant slope of the water uptake and applied suction line respectively. The value of $K(t) = 1.57 - 1.58 \times 10^{-3}t$ and τ is modeled as $\tau = -1.0\ (V_1)$. From the analogy of the Ohm's law, then the root resistance can be expressed by the following equation

$$(4) \quad R_1 = \frac{V_1 \times 137.3}{(\text{UPTAKE})}$$

Here the factor 137.3 is used to scale the root resistance to unity at the start of the photoperiod. The resistances R_1 and R_2 in the state Equation 2, are treated as a function of time. However, it is noted from Equation 4 that the root resistance depends upon the water potential V_1 in that component. Hence, it is postulated that a closed-loop feedback exists in the process.

The state equation for the stem and petiole component (Figure 1) at the node is presented as

$$(5) \qquad \frac{dV_2}{dt} = -[(V_2 - V_1) / (R_4 C_2) - (V_1 - V_2) / (R_2 C_2 + R_3 C_2)]$$

In the leaf, two components, leaf palisade and the spongy mesophyll were identified by Lang (6). They are also the site of evaporation and liquid to vapor transformation. The uniqueness of the process and the nonlinear relation between the potential and the vapor concentration for this component was developed by Rawlins (8). These concepts were incorporated in the model presented by Shirazi (9). The state equations for these components are as follows;

$$(6) \qquad \frac{dV_3}{dt} = -[(V_3 - V) / (R_5 C_3)]$$

for leaf palisade and for mesophyll component

$$(7) \qquad \frac{dV_4}{dt} = -[(V_4 - V_9) / (R_9 C_4) - (V_5 - V_4) / (R_7 C_4 + R_8 C_4) - (V - V_4) / (R_6 C_4)]$$

where $R_9 = R_g + R_s$ shown in Figure 1 in series. The mathematical expressions describing these resistances were presented by Shirazi (9) as

$$(8) \qquad R_g = -BV_4$$

and

$$(9) \qquad R_s = 500 \left\{\exp[-N(OPUT + 4.0)] - 1.0\right\} / [\exp(D_2 N - 1.0)]$$

where N and D_2 are constants.

In Figure 1 the potential change in the guard cell component is calculated at the node between R_8 and the nonlinear coupling. The potential change is given by the following state equation

$$(10) \quad \frac{dV_5}{dt} = -[(V_5 - V_4) / (R_7C_5 + R_8C_5)]$$

At the node between palisade and spongy mesophyll the potential varies as

$$(11) \quad V = [(V_2 / R_4) + (V_3 / R_5) + (V_4 / R_6)] / [(1/R_4) + (1/R_5) + (1/R_6)]$$

The transpiration rate analog is expressed at the point where flow leaves the system. This flow occurs through the potential across the stomata and is calculated as

$$(12) \quad I = (V_4 - V_9) / R_9$$

The rate of water intake (uptake rate) was simulated as flow across the potential between the solution culture (hypothetically maintained at zero potential) and the root potential component. The intake rate was governed by a closed loop consisting of the variable root resistance and the root potential. It was calculated as

$$(13) \quad INTAKE = -1.0\, V_1 / R_7$$

An analog computer mechanization of Equations 2 to 11 is presented in Figure 2. Equations defining the time-constants and multipliers are summarized in Table 2.

Simulation of the Stomatal Resistance Regulation Mechanism

Skidmore (12) reported a 5 to 7 minute delay in the stomatal action and water potential change in a cotton leaf and emphasized that future models should include time-delay and switching mechanisms in the feedback path. Phase differences in water uptake, transpiration and leaf density changes were reported by Shirazi (11). Based upon these results, a time-delay mechanism hysteresis was incorporated in the guard cell component. In order to simulate the damping oscillations during morning and sustained oscillations during evening another function, LIMIT, operating on the output of the hysteresis block was introduced. These

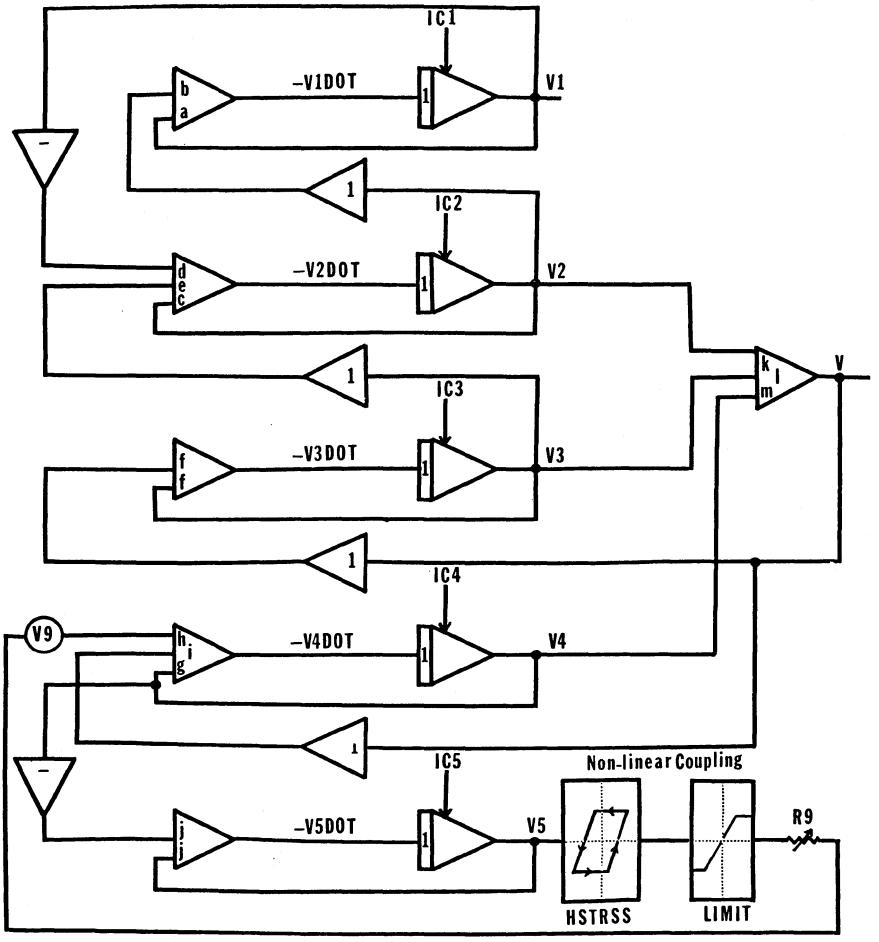

Figure 2. Analog computer mechanization of the transpiration model. Triangles with inputs of state variables and initial conditions are integrators. Open triangles with single input and unity gain are inverters.

CSMP blocks constitute the nonlinear coupling. Since both functions are nonlinear and multi-valued in the time domain, mathematical treatment of continuous function could not be applied. However, their use as a switching mechanism within the continuity of the system was utilized to transfer various parameters and the results of their interaction.

The expression of the stomatal resistance was obtained by operating

the nonlinearity upon the output of the guard cell potential V_5. The V_5 was obtained by integrating the state Equation 10 as follows:

$$(14) \qquad V_5 = \text{INTGRL}(IC_5, dV_5/dt)$$

where IC_5 is the assigned equilibrium potential of the guard cell at time = zero. Conditions on the size of increment of integration are discussed in Appendix 2. The validity of a hysteresis loop was documented by Shirazi (11). A hysteresis function V_{5H} was generated through the function generator block HSTRSS of the CSMP as

$$(15) \qquad V_{5H} = \text{HSTRSS}(IC_5, W_1, W_2, V_5)$$

where the IC_5 initial condition was as described earlier. The parameter arguments W1 and W2 are the width of hysteresis loop (9). The hysteresis function is a history element and its output depends upon both the present input and the past value of the output. At time equal to zero it set the value of output equal to the IC_5. Thereafter, output is computed in accordance with the following conditions (See Figure 3):

$$V_{5H} = V_5 - W_2, (V_5 - V_{5_{n-1}}) \geq 0, V_{5H_{n-1}} \leq V_5 - W_2$$

$$V_{5H} = V_5 - W_1, (V_5 - V_{5_{n-1}}) \leq 0, V_{5H_{n-1}} \geq V_5 - W_1$$

The output V_{5H} is further controlled by the limits on its operation through a soft nonlinearity, function generator LIMIT, of the CSMP in the following way:

$$(16) \qquad \text{OPUT} = \text{LIMIT}(K_2, -4.0, V_{5H})$$

where OPUT is the name of the function output, and K_2 and —4.0 are the lower and the upper bound parameters respectively, and V_{5H} is the input expression. This routine produces an output equal to V_{5H} according to the restrictions imposed by parameters (K_2, —4.0) in such a way that when V_{5H} is equal to or less than K_2, the output is set equal to K_2.

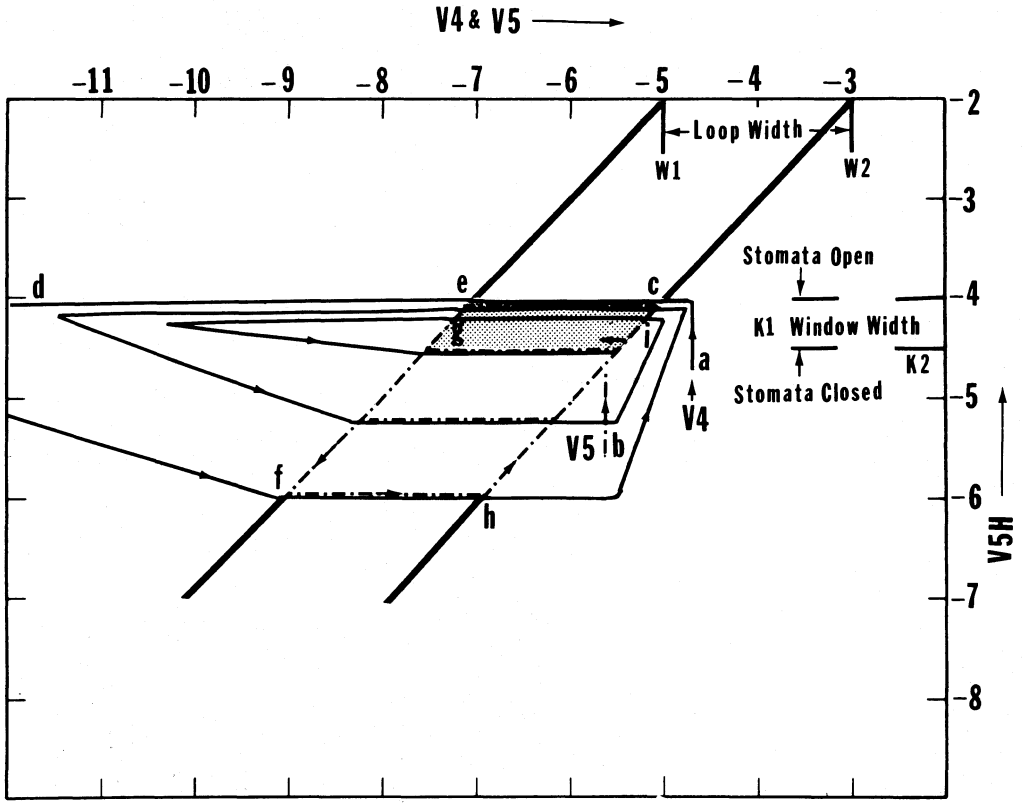

Figure 3. Hypothetical Interaction of V_4, V_5 and V_{5H} variables, as affected by the magnitude of the parameters W_1, W_2 and window width (K_1).

If V_{5H} is equal to or greater than —4.0, the V_{5H} output is set equal to —4.0. For intermediate values the OPUT remains equal to V_{5H}.

In generating the lower and upper bounds of the LIMIT, the upper potential was maintained at—4.0 corresponding to the experimental results of Shirazi (9). Additionally, the lower bound K_2 was gradually changed from —4.0 to —4.25 by following time-variant mathematical expressions:

$$(17) \qquad Y_1 = -4.0\ [\exp(Zt)]$$

$$(18) \qquad K_1 = -0.25\ [\{\exp[-M(Y_1 + 4.0)]\} - 1.0]\ /\ [\exp(DM - 1.0)]$$

$$(19) \qquad K_2 = -4.0 + K_1$$

where D, Z and M are constants.

Finally, based upon the value of the output of Equation 16 the potential dependent stomatal resistance R_s was calculated as

$$(20) \qquad R_S = [\,500\ \{\exp -N(OPUT + 4.0)]\ \} - 1.0\ ]\ /[\exp(D_2N - 1.0)]$$

where D2 and N are constant (see Appendix 1). It is seen that when OPUT is equal to —4.0 the R_s is equal to zero and stomata are open and when OPUT is equal to —4.25, R_s is equal to 500 units and the stomata are closed.

Since it is not intuitively obvious how the foregoing functions simulate the operation of stomata, the following graphical analysis is offered.

Figure 3 illustrates a typical scan showing how V_5 follows V_4 and how V_{5H} is generated. The variable V_5 traces along the right diagonal after moving vertically to it. This initial condition is the only time V_5 is outside the bounds of this diagonal. The reason for this initial condition is described later. The points *a* and *b* represent initial conditions at this point, $V_{5H} \geqslant -4.0$ and the stomata are open, causing V_4 to drop rapidly, going from *c* to *d* and beyond. V_5 follows V_4 to the lower limit of the hysteresis bound *e*, and then follows this bound towards *f*, changing V_{5H} as it traverses the window. When V_5 passes point g, $V_{5H} \leqslant K_2$ and the

stomata are closed. V_4 then recovers and moves towards *f*, overtaking V_5 and moving rapidly past *h*. V_5 follows to *h*, and is then constrained to follow the upper bound (right diagonal) of the hysteresis loop towards *c*. As V_5 passes *j*, $V_{5H} < K_2$ and stomata start to open, initiating a new cycle.

Results and Discussion

The graphical results of the simulation can be obtained by the CSMP instruction PRTPLT for several variables. Numerical values of associated variables can be printed on the side of the graph. One such output V_4 is presented in Figure 4. The pattern of simulation results, the periodic relations, and the relative magnitude of the changes in the potential of different plant components are within acceptable limits of the data reported by Shirazi (9, 11).

During the early stage of model development, sustained and symmetrical oscillations were obtained by the use of the hysteresis function alone. These oscillations were similar to that simulated by Cowan (2). However, the data and the time-lapse movies of the leaf response obtained by Shirazi (11) showed damping oscillations in the morning phase and sustained oscillations during the evening phase. In the present model therefore, the constraints discussed above on the V_{5H} were set to simulate the morning and the evening oscillations.

A hypothetical combination of parameters interacting on the nonlinearity was presented by Shirazi (9). It was observed that for a given value of W_1 and W_2 changing the limits on V_{5H}, the system response adjusted itself to over-damped or under-damped oscillations. The physical significance of these parameters and their effect on the output of potential in different plant components was documented by Shirazi (9).

In the present model a function TLAPS (for the elapsed time) was defined late in the photoperiod as

$$\text{(21)} \qquad \text{TLAPS} = (\text{TIME} - 520)$$

Readjustment of the parameters was made to simulate the conditions necessary for the evening oscillations (see program listing Appendix 1). Evening oscillations have been reported by several workers (3, 11, 12). Skidmore (12) Parsons (7), and Shirazi (10) reported 3- to 6-fold increase in the root resistance during the photoperiod. In the computer output it was observed that the system becomes unstable at higher root resistance. However, the magnitude of the instability was too small to initiate oscillations in the water-based dynamic processes. To simulate the evening cycling two parameters, the limits on the V_{5H} and the arguments

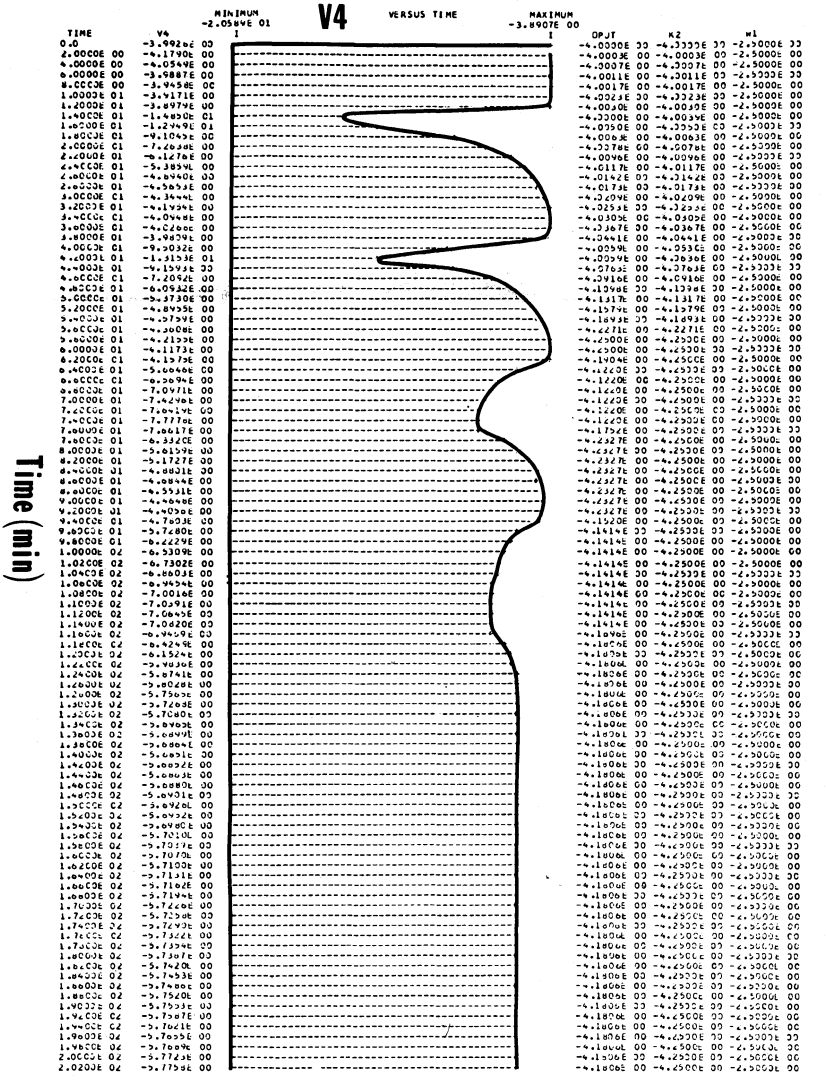

Figure 4. A CSMP computer output of variable V, as a function of time showing early-day oscillations. Tabulated output is called-out in the program and can be varied at will.

of the hysteresis loop were readjusted. The value of K_2 was reduced by about 40 percent of the steady-state condition. This was achieved by the following mathematical functions:

$$(22) \quad Y_2 = [-4.0 - 0.25 \{\exp[(C)(TLAPS)] - \exp(CZ_2)\}] / [1 - \exp(CZ_2)]$$

$$(23) \quad K_1 = [-0.15 \{\exp[-M(Y_2 + 4.0)] - 1.0\}] / [\exp(DM) - 1.0]$$

$$(24) \quad K_2 = -4.0 + K_1$$

where C and Z_2 are constant. Similarly, it was necessary to relocate and redefine the hysteresis width by changing the parameters W_1 and W_2 as a function of time.

This was achieved by the following mathematical functions

$$(25) \quad W_1 = -2.5 \{\exp[1.59 \times 10^{-2} (TLAPS)]\}$$

$$(26) \quad W_2 = -1.0 \{\exp[2.73 \times 10^{-2} (TLAPS)]\}$$

FORTRAN branching and conditional transfers were made in the NOSORT section of the CSMP program to obtain final values of the parameters and run control (see Appendix 1). For rapidly rising and falling functions such as the state variables in the present model variable step-size method of integration was found to consume considerable time on the central processing unit of the computer. Therefore, the Trapezoidal method was used to integrate the state equations. It was found that the integration interval must be smaller than the smallest time-constant in the analog RC model (Appendix 2).

Probably at a certain stage of model-building the modeler has a prior agreement to simulate his results. Modeling and simulation techniques have some inherent credibility problems. But the merit of systems approach, such as present in this paper, lies in the appreciation of these limitations. Simulation currently represents a philosophy of computing which emphasizes the interpretation of the processes interconnected by a network of rational cause-effect relationships. The present model should find utility in laboratories when kinetics of water flow through

plants is under study. The model is general and is readily adaptable to conditions other than those reported here.

Some second thoughts on modeling are offered. The present system with the lumped constants and macro level conceptualization can be modeled either by electric or hydraulic analog. The electric model used herein can be solved directly by analog computer or digital computer (as was employed). There is merit to the electric analog here since the immediate predecessors in the literature have used electric analog models. However, the authors question the use of electric analog indefinitely. At some time in the future, understanding will have advanced to a point where hydraulic modeling will be more satisfying conceptually. It will be increasingly difficult to interpret new mechanisms from *in vivo* observations if R-C models are continued indefinitely. R-C network models represent only a small part of the total set of models based on ordinary differential equations and the complex mechanisms within plants will require more flexible models. It is therefore suggested that future modelers should think along the lines of hydraulic models which also yield similar differential equations, and can easily be solved by digital simulation. These models are more easily developed from the basic understanding of the biological processes involved and the computer simulations results are more easily interpreted and interfaced to models of micro processes.

Literature Cited

1. Barrs, H.D., and B. Klepper. 1968. Cyclic Variations in Plant Properties Under Constant Environmental Conditions. Physiol. Plant. 21:711-730.
2. Cowan, I.R. 1972. Oscillations in Stomatal Conductance and Plant Functioning Associated with Stomatal Conductance: Observations and a Model. Planta. 106:185-219.
3. Hopmans, P.A.M. 1971. Rhythms in Stomatal Opening of Bean Leaves. Meded. Landbouwhoogeschool. 71(3):1-86.
4. IBM, 1969. 05/360. Continuous System Modeling Program: User's Manual. Application Description H20-0367-3.
5. Konig, H.E., Y. Tokad, and H.K. Kesavan. 1967. Analysis of Discrete Physical Systems. McGraw-Hill Inc., New York.
6. Lang, A.R.C., B. Klepper, and M.J. Cumming. 1969. Leaf Water Balance During Oscillation of Stomatal Aperture. Plant Physiol. 44:826-830.
7. Parsons, L.R., and P.J. Kramer. 1974. Diurnal Cycling in Root Resistance to Water Movement. Physiol. Plant. 30:19-23.
8. Rawlins, S.L. 1963. Resistance to Water Flow in the Transpiration Stream in I. Zelitch (ed) Stomata and Water Relation in Plants. p. 69-85. Conn. Agric. Exp. Sta. Bull. 664.
9. Shirazi, G.A., J.F. Stone, and C.M. Bacon. 1976. Oscillatory Transpiration in a Cotton Plant. II. A Model. J. Exp. Bot. 27:619-633.
10. Shirazi, G.A., J.F. Stone, L.I. Croy, and G.W. Todd. 1975. Changes in Root Resistance as a Function of Applied Suction, Time of Day, and Root Temperature. Physiol. Plant. 33:214-218.
11. Shirazi, G.A., J.F. Stone, and G.W. Todd. 1976. Oscillatory Transpiration in a Cotton Plant. I. Experimental Characterization. J. Exp. Bot. 27:608-618.
12. Skidmore, E.L., and J.F. Stone. 1964. Physiological Role In Transpiration Rate of the Cotton Plant. Agron. J. 56:405-410.

Appendix 1.

```
        ****CONTINUOUS SYSTEM MODELING PROGRAM****

                    *** VERSION 1.3 ***

      INITIAL
   TITLE    SIMULATION OF TRANSPIRATION STREAM IN A COTTON PLANT
      CONSTANT R3=2.5,R4=2.5,R5=2.5,R6=2.5,R7=2.5,...
   E=200., C1=1.66E-01, C2=8.66E-03, C3=0.350, C4=0.3500,...
R8=3000.0,B=-3.0,A=0.9605,N=3.0, C5=3.50E-03,Z2= 55.0,C=0.1
   INCON  IC1= -0.4964,IC2=-1.9928,IC3=-2.9928,IC4=-3.9928,IC5=-7.5
      PARAMETER   W1=-2.5,W2=-1.0,Z=1.0625E-03,SW=1., M=20.0
      V9= -F
      V5H1=-7.5
   DYNAMIC
      R2=  R1T
      R1T=    -(V1/UPTAKE)*137.3
      INTAKE=  -(1.0/R1T)*V1
      KSUBT=      (1.57394-0.00158*(TIME))
      TAU=   -1.0*V1
      UPTAKE=   EXP(2.3026*(A+KSUBT*TAU))
      RSUBG=  B*V4
      R9=  RSUBG+RSUBS
      I=  (V4-V9)/R9
   V= (V2/R4+V3/R5+V4/R6)/(1.0/R4+1.0/R5+1.0/R6)
   V1DOT= -((V1-V2)/(R2*C1+R3*C1)+V1/(R1T*C1))
   V2DOT=  -((V2-V)/(C2*R4)-(V1-V2)/(C2*R2+C2*R3))
   V3DOT=  -((V3-V)/(C3*R5))
   V4DOT=  -((V4-V9)/(C4*R9)-(V5-V4)/(C4*R7+C4*R8)-...
   (V-V4)/(C4*R6))
      V5DOT=  -((V5-V4)/(C5*R7+C5*R8))
      V1=  INTGRL(IC1,V1DOT)
      V2=  INTGRL( IC2,V2DOT)
      V3=   INTGRL(  IC3, V3DOT)
      V4=  INTGRL( IC4,V4DOT)
      V5=  INTGRL(IC5,V5DOT)
   V5H=  HSTRSS( V5H1,W1,W2,V5)
      VD=  (V3+V4)/2.0
   NOSORT
      TLAPS=  (TIME-520.0)
   IF (TIME.GE.520.0) GO TO 20
   IF  (SW.EQ.0.0)  GO TO 20
      Y1=   -4.0*(EXP(Z*(TIME)))
   IF( Y1.LE.-4.25) Y1= -4.25
      D=0.25
      K1=   -0.25*((EXP(-M*(Y1+4.0)))-1.0)/(EXP(D*M)-1.0)
      K2= -4.0+K1
   OPUT=  LIMIT(K2,-4.0,V5H)
   D2=  -(K2+4.0)
   RSUBS= 500.00/((EXP(D2*N))-1.0)*((EXP(-N*(OPUT+4.0)))-1.0)
   GO TO 3
```

```
      20  Y2= -4.0-0.25*((EXP(C*TLAPS)-EXP(C*Z2))/(1.0-EXP(C*Z2)))
             IF (Y2.GE.-4.02) Y2=-4.02
          SW=0.0
          W1=  -2.5*(EXP(1.5917E-02*TLAPS))
             IF (W1.LE.-6.0) W1=-6.0
          W2=  -1.0*(EXP(2.7347E-02*TLAPS))
             IF (W2.LE.-3.0) W2= -3.0
             M=0.1
             D=0.23
             K1=   -0.15*((EXP(-M*(Y2+4.0)))-1.0)/(EXP(D*M)-1.0)
             K2= -4.0*K1
          OPUT=  LIMIT(K2,-4.0,V5H)
             D2=  -(K2+4.0)
          RSUBS=  500.0/((EXP(D2*N))-1.0)*((EXP(-N*(OPUT+4.0)))-1.0)
       3  CONTINUE
          TERMINAL
             METHOD  TRAPZ
          TIMER    FINTIM=   720.0, DELT= 1.5E-02, OUTDEL=  2.0
          PRTPLT  V1(R1T),V2,V3,V4(OPUT,K2,W1),V5(V5H,Y2,W2),VD,I,INTAKE,...
             R9(RSUBS,RSUBG)
         END
          STOP

OUTPUT VARIABLE SEQUENCE
V9      V5H1    TAU     KSUBT   UPTAKE R1T     R2      V1DOT   V1      V
V2DOT   V2      V3DOT   V3      RSUBG  R9      V4DOT   V4      V5DOT   V5
INTAKE  I       V5H     VD      TLAPS  ZZ0006  Y1      Y1      D       K1
K2      OPUT    D2      RSUBS   Y2     Y2      SW      W1      W1      W2
W2      M       D       K1      K2     OPUT    D2      RSUBS

PARAMETERS NOT INPUT OR OUTPUTS NOT AVAILABLE TO SORT SECTION***SET TO ZERO***
RSUBS

 OUTPUTS     INPUTS   PARAMS  INTEGS + MEM BLKS  FORTRAN  DATA CDS
 52(500)  119(1400)  31(400)   5+  0=  5(300)   52(600)     11

          ENDJOB
```

Appendix 2

The Limitation upon DELT in the Method of Integration

The continuous System Modeling Program (CSMP) language offers several optional methods of integration to its users. The methods are broadly classified as either fixed-step or variable-step size routines. In view of the fact that a large number of integration steps were required for the entire photoperiod, some sophistication was sacrificed to make overall run economical.

The simulation runs were tried using variable-step and the fixed-step methods. The Trapezoidal method was finally adapted. The method does not use a corrector equation, but uses the estimation equation only, along with the predictor equation
The predictor;

$$(27) \qquad Y^{P}_{(t+\Delta t)} = Y_t + X_t \Delta t, \text{ where } X_t = \frac{dy}{dt}\Big|_t$$

and the estimate;

$$(28) \qquad Y_{(t+\Delta t)} = Y_t + (X_t + X_{t+\Delta t}) \frac{\Delta t}{2}$$

The estimate uses the average of the derivatives calculated for time 't' and $(t + \Delta t)$, where $(t + \Delta t)$ is based upon predictor value $Y^{p}_{(t+\Delta_t)}$. This computation, therefore, involves two calls to update at each DELT.

The nodal analysis of the RC circuit showed that it is critical to choose a proper DELT for the integration routine. The importance of the DELT can be shown by a simple RC block as in Figure 5. Let the node be at V_1 and let $V_2 = -E$. As before, the flow of current coming into the node is positive and the flow going out of the node is negative. Thus, since $V_2 = -E$, and for small changes in voltage at each iteration we have

$$(29) \qquad \frac{\Delta V_1}{\Delta t} = \frac{-1}{RC} (V_1 + E)$$

or

$$(30) \qquad \Delta V_1 = \frac{-\Delta t}{RC} (V_1 + E)$$

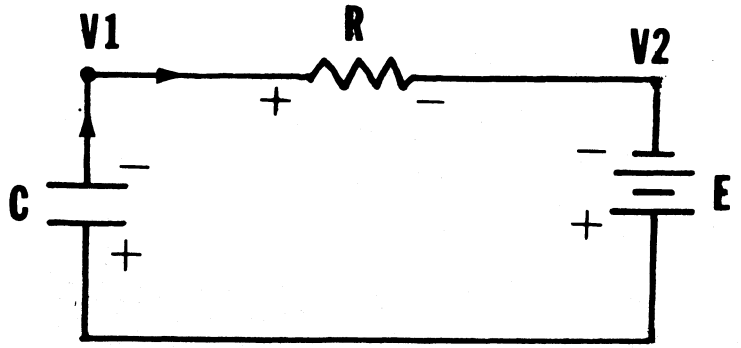

Figure 5. A basic component of an R-C circuit explaining the procedure for writing state equations.

The boundary conditions are such that $V_1 = 0$. Therefore, the first iteration gives

$$(31) \qquad {}^{1}Y_{(t+\Delta t)} = 0 + \frac{-\Delta t}{RC}(0 + E)$$

and the second iteration gives

$$(32) \qquad {}^{2}Y_{(t+\Delta t)} = \frac{-\Delta t}{RC}E + \frac{-\Delta t}{RC}\left(\frac{-\Delta t}{RC}E + E\right)$$

or

$$(33) \qquad \frac{{}^{2}Y_{t+\Delta t}}{E} = \frac{\Delta t}{RC}\left(\frac{\Delta t}{RC} - 2\right)$$

$$(34) \qquad \left(\frac{\Delta t}{RC} - 2\right) = 0, \text{ or } \Delta t = 2RC$$

Hence, the DELT for integration would be $< 2RC$ so that the output will carry the proper sign. Unlike SIMP and MILNE methods, the TRAPZ method of integration does not use a corrector term, therefore, it is advisable to use a somewhat smaller DELT than the limiting value. This analysis is true for the RECT method of integration also.

Appendix 3

Stability of the Model

The model depicts a nonlinear system. The primary control feature is characterized by a nonlinear coupling represented by the hysteresis block in Figure 1. To establish the overall stability of the model, it was necessary to examine the nature of the eigenvalues of the system matrix using the coefficients of state variables V_1 to V_5. To establish the system matrix, the state equations 2, 5, 6, 7, 10, and 11 were expanded to separate the variables as follows.

$$(35) \quad \frac{dV_1}{dt} = \frac{-V_1}{C_1R_1} + \frac{V_2}{C_1(R_2+R_3)} - \frac{V_1}{C_1(R_2+R_3)}$$

$$(36) \quad \frac{dV_2}{dt} = \frac{V_1}{C_2(R_2+R_3)} - \frac{V_2}{C_2(R_2+R_3)} - \frac{V_2}{C_2R_4} + \frac{V_2}{C_2(R_4)^2\left(\frac{1}{R_4}+\frac{1}{R_5}+\frac{1}{R_6}\right)} + \frac{V_3}{C_2R_4R_5\left(\frac{1}{R_4}+\frac{1}{R_5}+\frac{1}{R_6}\right)} + \frac{V_4}{C_2R_4R_6\left(\frac{1}{R_4}+\frac{1}{R_5}+\frac{1}{R_6}\right)}$$

$$(37) \quad \frac{dV_3}{dt} = \frac{V_2}{C_3R_4R_5\left(\frac{1}{R_4}+\frac{1}{R_5}+\frac{1}{R_6}\right)} + \frac{V_3}{C_3(R_5)^2\left(\frac{1}{R_4}+\frac{1}{R_5}+\frac{1}{R_6}\right)} + \frac{V_4}{C_3R_5R_6\left(\frac{1}{R_4}+\frac{1}{R_5}+\frac{1}{R_6}\right)} - \frac{V_3}{C_3R_5}$$

$$(38)\quad \frac{dV_4}{dt} = \frac{V_2}{C_4R_4R_6\left(\frac{1}{R_4}+\frac{1}{R_5}+\frac{1}{R_6}\right)} + \frac{V_3}{C_4R_5R_6\left(\frac{1}{R_4}+\frac{1}{R_5}+\frac{1}{R_6}\right)}$$

$$+ \frac{V_4}{C_4(R_6)^2\left(\frac{1}{R_4}+\frac{1}{R_5}+\frac{1}{R_6}\right)} - \frac{V_4}{C_4R_6} + \frac{V_5}{C_4(R_7+R_8)}$$

$$- \frac{V_4}{C_4(R_7+R_8)} + \frac{V_9}{C_4(R_g+R_s)} - \frac{V_4}{C_4(R_g+R_s)}$$

$$(39)\quad \frac{dV_5}{dt} = \frac{V_4}{C_5(R_7+R_8)} - \frac{V_5}{C_5(R_7+R_8)}$$

$$(40)\quad V = \frac{\left(\frac{V_2}{R_4}+\frac{V_3}{R_5}+\frac{V_4}{R_6}\right)}{\left(\frac{1}{R_4}+\frac{1}{R_5}+\frac{1}{R_6}\right)}$$

The coefficients of the variables were collected and are shown in Table 1. Numerical values of the matrix elements were calculated for three states of the system, namely (1) charging cycle, (2) discharging cycle, and (3) steady-state condition. All eigenvalues were found to be real and negative. This means that the model is stable in the time domain.

Abstract

A computer simulation model of the transpiration process in a cotton plant growing in solution culture in a constant environment chamber is presented. The model accounts for the cyclic variations in transpiration during the entire length of a light period. The 'lumped parameters' approach for modeling the transpiration process is based upon the experimental results of response characteristics of a cotton plant exposed to a severe evaporative demand.

The model was written in the simulation language Continuous System Modeling Program (CSMP1-0 S/360). The Trapezoidal method of integration was employed to this circuit. This method is adapted to transient functions. The integration interval was found to be limited by the value of the smallest time-constant in the circuit.

A network analysis of the system showed that oscillation could not be caused by the RC makeup of the model so oscillation was due only to the coupling between guard cell potential and stomatal resistance.

Table 1. A Symmetrical Matrix of 5x5 Elements Used for the Calculation of Eigenvalues

29	V_1	V_2	V_3	V_4	V_5
C_1	$-\frac{1}{R_1C_1} - \frac{1}{C_1(R_2+R_3)}$	$\frac{1}{C_1(R_2+R_3)}$	0	0	0
C_2	$\frac{1}{C_2(R_2+R_3)}$	$-\frac{1}{C_2(R_2+R_3)} - \frac{1}{C_2R_4} + \frac{1}{C_2(R_4)^2(\frac{1}{R_4}+\frac{1}{R_5}+\frac{1}{R_6})}$	$\frac{1}{C_2R_4R_5(\frac{1}{R_4}+\frac{1}{R_5}+\frac{1}{R_6})}$	$\frac{1}{C_2R_4R_6(\frac{1}{R_4}+\frac{1}{R_5}+\frac{1}{R_6})}$	0
C_3	0	$\frac{1}{C_3R_4R_5(\frac{1}{R_4}+\frac{1}{R_5}+\frac{1}{R_6})}$	$\frac{1}{C_3(R_5)^2(\frac{1}{R_4}+\frac{1}{R_5}+\frac{1}{R_6})} - \frac{1}{C_3R_5}$	$\frac{1}{C_3R_5R_6(\frac{1}{R_4}+\frac{1}{R_5}+\frac{1}{R_6})}$	0
C_4	0	$\frac{1}{C_4R_4R_6(\frac{1}{R_4}+\frac{1}{R_5}+\frac{1}{R_6})}$	$\frac{1}{C_4R_5R_6(\frac{1}{R_4}+\frac{1}{R_5}+\frac{1}{R_6})}$	$\frac{1}{C_4(R_6)^2(\frac{1}{R_4}+\frac{1}{R_5}+\frac{1}{R_6})} - \frac{1}{C_4R_6} - \frac{1}{C_4(R_7+R_8)} - \frac{1}{C_4(R_8+R_8)}$	$\frac{1}{C_4(R_7+R_8)}$
C_5	0	0	0	$\frac{1}{C_5(R_7+R_8)}$	$-\frac{1}{C_5(R_7+R_8)}$

Table 2. The Time-Constants and the Constant Multipliers for the Analog Computer Diagram of Figure 2.

(Note that some resistances are not constant. See text.)

$$a = \left[\frac{1}{R2C1 + R3C1} + \frac{1}{R1C1}\right]$$

$$b = \left[\frac{1}{R2C1 + R3C1}\right]$$

$$c = \left[\frac{1}{R4C2} + \frac{1}{R2C2 + R3C2}\right]$$

$$d = \left[\frac{1}{R2C2 + R3C2}\right]$$

$$e = \left[\frac{1}{R4C2}\right]$$

$$f = \left[\frac{1}{R5C3}\right]$$

$$g = \left[\frac{1}{R9C4} + \frac{1}{R7C4 + R8C4} + \frac{1}{R6C4}\right]$$

$$h = \left[\frac{1}{R9C4}\right]$$

$$i = \left[\frac{1}{R6C4}\right]$$

$$j = \left[\frac{1}{R7C5 + R8C5}\right]$$

$$k = \left[\frac{1/R4}{1/R4 + 1/R5 + 1/R6}\right]$$

$$l = \left[\frac{1/R5}{1/R4 + 1/R5 + 1/R6}\right]$$

$$m = \left[\frac{1/R6}{1/R4 + 1/R5 + 1/R6}\right]$$